

LEGRI OPERATIONS. DETECTORS AND DETECTOR STABILITY

V. REGLERO¹, F. BALLESTEROS³, P. BLAY¹, E. PORRAS², F. SÁNCHEZ² and
J. SUSO¹

¹ *GACE, Instituto de Ciencias de los Materiales, Universidad de Valencia, P.O. Box 2085, 46071 Valencia, Spain*

² *Instituto de Física Corpuscular, Spanish Council of Scientific Research - University of Valencia, Edificio de Institutos de Paterna, P.O. Box 2085, E-4 6071 Valencia, Spain*

³ *Centro de Astrobiología (CAB), Instituto Nacional de Técnica Aeroespacial (INTA), Ctra. de Ajalvir Km. 14, Torrejón de Ardoz, Madrid, Spain*

Abstract. Two years after launch (04.21.97), LEGRI is operating on Minisat-01 in a LEO orbit. The LEGRI detector plane is formed by two type of gamma-ray solid state detectors: HgI₂ and CdZnTe. Detectors are embedded in a box containing the FEE and DFE electronics. This box provides an effective detector passive shielding. Detector plane is multiplexed by a Coded Aperture System located at 54 cm and a Ta Collimator with a FCFOV of 22° and 2° angular resolution. The aim of this paper is to summarize the detector behaviour in three different time scales: before launch, during the in-orbit check-out period (IOC), and after two years of routine operation in space. Main results can be summarized as follows:

A large fraction of the HgI₂ detectors presented during LEGRI IOC very high count ratios from their first switch-on (May 1997). Therefore, they induced saturation in the on-board mass memory. After some unsuccessful attempts to reduce the count ratios by setting up different thresholds during LEGRI IOC, all of them were switched off except nine detectors in column 4, with a higher degree of stability.

Oppositely, the 17 CdZnTe detectors present a remarkable stability in both their count-ratios and spectral shapes. Details about CdZnTe ground energy calibration, in-flight calibration (using the Crab) and detector stability are discussed hereafter. Detector efficiency function has been computed with the fixed flight threshold used within the calibrated energy range (20–80 KeV). It presents a maximum at 60 KeV, and decreasing efficiencies in the lower and upper energy range ends. Both, non-linear threshold cutting and the drop in the detector efficiency explain the CdZnTe computed operational efficiency response.

1. Introduction.

LEGRI design philosophy and goals were both linked to early stages of the Imager development for the ESA mission INTEGRAL. By the time LEGRI proposal was written (1992) most of the LEGRI team members were also working in the definition of the Imager, one of the main instruments for the ESA M2 mission.

The INTEGRAL Imager baseline configuration was conceived upon the use of CsI scintillators of different thickness located in three different layers. By then (1993), new technologies of solid state detectors began to be available: the HgI₂, the CdTe and the very new CdZnTe. All of them with a very remarkable property,



Astrophysics and Space Science is the original source of this article. Please cite this article as: *Astrophysics and Space Science* **276**: 239–253, 2001.
© 2001 Kluwer Academic Publishers. Printed in the Netherlands.

their capability to work at room temperature. For the Imager designers there were clear advantages in implementing a detector layer of this type, besides the existing CsI detector planes. On the scope of a common period of operations for INTEGRAL and XMM, the capability of the Imager to go up to 20 KeV by using solid state detectors was considered as a unique opportunity to connect the upper XMM energy range with the lower end of the INTEGRAL Imager. Scientific benefits were obvious.

In coincidence with these early stages of the INTEGRAL development, the Instituto Nacional de Tecnologías Aeroespaciales (INTA) released a Call for Ideas for an instrument to fly on the MINISAT-01, beside the other two instruments (EURD – Espectrógrafo Ultravioleta extremo para la observación de la Radiación Difusa– and CPLM – Comportamiento de Puentes Líquidos en Microgravedad) already selected in early project phases. With a MINISAT-01 200 kg total mass, LEGRI should not surpass a total mass of 20–30 kg. Development time was also short, its delivery stated for the beginning of 1996. This implied only three years for instrument development, test and flight qualification.

The proposal submitted by the LEGRI team was a hard X-ray and soft Gamma-ray Imager as a demonstrator of technology for the HgI₂ solid state detectors, shadowed by a 5 × 5 MURA mask as a spatial signal multiplexing system. (Ballesteros *et al.*, 1998). The instrument name, Low Energy Gamma Ray Imager (LEGRI), comes from this definition. Restrictions in terms of mass (20–30 kg), power (20 w) and mass memory allocation (10 Mb) from the MINISAT-01 project team imposed severe constraints on the LEGRI definition parameters. The final solution adopted was a square detector plane of 100 HgI₂ detectors 1 cm² area and 0.5 mm thickness each, embedded in a box containing the FEE and associated DFE electronics.

The box was designed to provide the required stiffness to the Detector Plane (DP) and associated electronics, as well as a passive shielding for both cosmic and Earth trapped particle interactions. In order to achieve a perfect matching between the FCFOV defined by the mask assembly and the total LEGRI FOV, a Ta Collimator was located on top the DP. The LEGRI FOV is 22°, with an angular resolution of 2.2°. The detector plane, FEE, DFEE, collimator and passive graded shield define the Detector Unit (DU).

LEGRI scientific goals, apart from the above referred technological issues, aimed to perform a continuum monitoring of strong variable sources at the level of 10 mCrab sensitivity in 10⁵ sec at 3 sigma level. The scope of this paper is to report LEGRI detector development and its in-orbit operational behaviour; we will not go further in the definition of the Detector Unit. More details on both DU and other LEGRI systems can be found in Reglero *et al.*, 1997. Location of the LEGRI units in the MINISAT-01 Payload Module are displayed in Figure 1. Non-shadowed boxes correspond either to EURD or CPLM instruments.

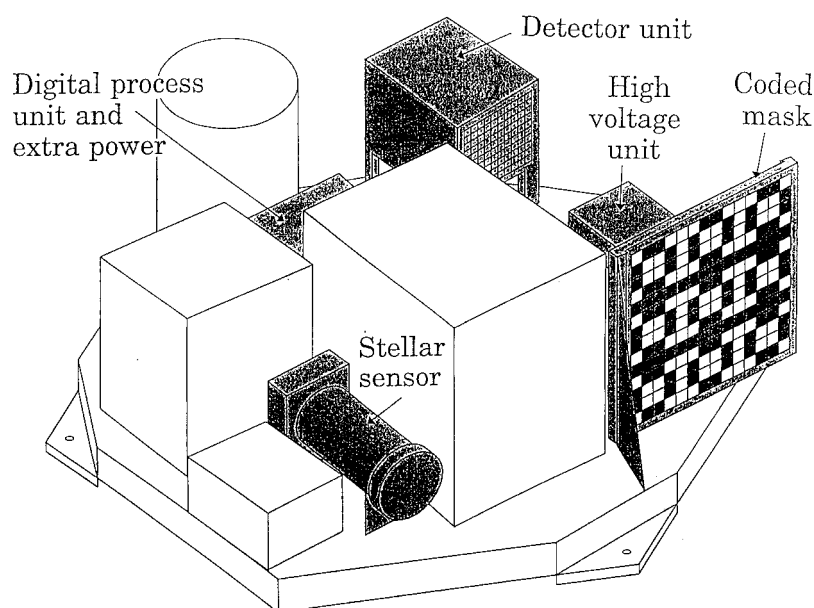


Figure 1. LEGRI units on MINISAT-01 Payload Module.

2. LEGRI hardware flight configuration

During the detector plane design and manufacturing (1993-96), two main events had a strong impact on the LEGRI hardware development: the UK withdraw from the INTEGRAL Imager and the inability of the CIEMAT crystal builders to deliver 100 HgI_2 detectors of 1 cm^2 . Let us start by the end.

Two years after starting the LEGRI project (late 1994) it was clear that CIEMAT was not able to deliver to the consortia the required 100 good quality HgI_2 detectors 1 cm^2 each. Finally, 100 crystals with a 30 cm^2 collecting area were delivered to RAL in 1995 for integration. This degradation on the collecting area had a serious impact on the LEGRI scientific goals, with a reduction of $1/3$ in its detecting area. Looking for an issue to this very undesirable situation, an offer came from CalTech, to implement 20 new technology CdZnTe 1 cm^2 and 1.5 mm thickness each. This is how we decided to replace 20 HgI_2 detectors by two rows of 10 CdZnTe detectors, located in both DP ends. The polarisation voltage was chosen to maximise the output of both kinds of detectors HgI_2 and CdZnTe .

Since its inception, we assumed the use in LEGRI of the existing electronics under development at RAL for the Imager. The UK withdraw from the INTEGRAL Imager (renamed IBIS) implied a halt in the FEE development. Electronics development suffered from this new situation and, as a result, a less performant electronic was built. Electronic noise increased from the expected 900e to 1400e

in the flight configuration. Thus, thresholds were increased to prevent electronic noise intrusion.

During the final DP assembly and testing at Birmingham University, one of the CdZnTe detectors broke down. At the same time, we discovered that the first detector in each of the 10 rows presented a very strong electronic noise related with some misworking in the electronic readouts. Consequently, the final DP hardware in flight configuration was 17 CdZnTe detectors of 1 cm² and 1,5 mm thickness each, plus 72 HgI₂ detectors 0,5 mm thickness each with a collecting area of 22 cm². This flight configuration presented an advantage with respect to the initial design ideas on having two different kinds of detectors. Oppositely, the total collecting area dropped from 100 cm² to 39 cm². In some way LEGRI was then improved as a technological demonstrator, but it lost a significant fraction of its scientific capabilities as an astronomical instrument.

3. In-Orbit Checkout

LEGRI was switched-on for the first time on May 21st 1997, once the MINISAT-01 IOC at satellite level was finished. The in-orbit LEGRI checkout covers the period between May 21st and September 1997, when the Crab Nebulae observations finished.

The switching-on was done sequentially: Data Processing Unit and Star Sensor (SS) first, maintaining the detector polarisation off in the Detector Unit. The house-keeping data (HK) received during the first two days of operations were in accordance with their design values, showing the good behaviour of all LEGRI subsystems (see Suso *et al.*, 2001, in this volume). The SS recognised Deneb and all the stars up to magnitude 5.5 in the Deneb surroundings. More details on SS operational performances and its pointing reconstruction capabilities can be found in Blay *et al.* (2001, in this volume).

Last step on the LEGRI IOC was to switch on the High Voltage Unit to polarise the detectors at 280V. The telemetry received next day showed that the 10MB of mass memory available for LEGRI on Minisat-01 was completely full in only three orbits. Data from the rest of the day (13 orbits) were lost. The analysis of the downloaded data showed unexpected high count ratios in nearly all the HgI₂ detectors. Strong intrusion of electronic noise produced very fast memory saturation. Figure 2 displays the count ratio for the 9 HgI₂ detectors located in Column 1 in 49 minutes integration time versus energy channel. All histograms reveal the presence of strong electronic noise peaks between channels 500 and 1000. Electronic noise dominates the total count ratio at lower channels. The mass memory was, consequently, saturated very fast.

Once the problem was identified, new patch commands were sent with higher thresholds trying to avoid the intrusion of electronic noise. We also tried to test different operational configurations switching on and off different combinations

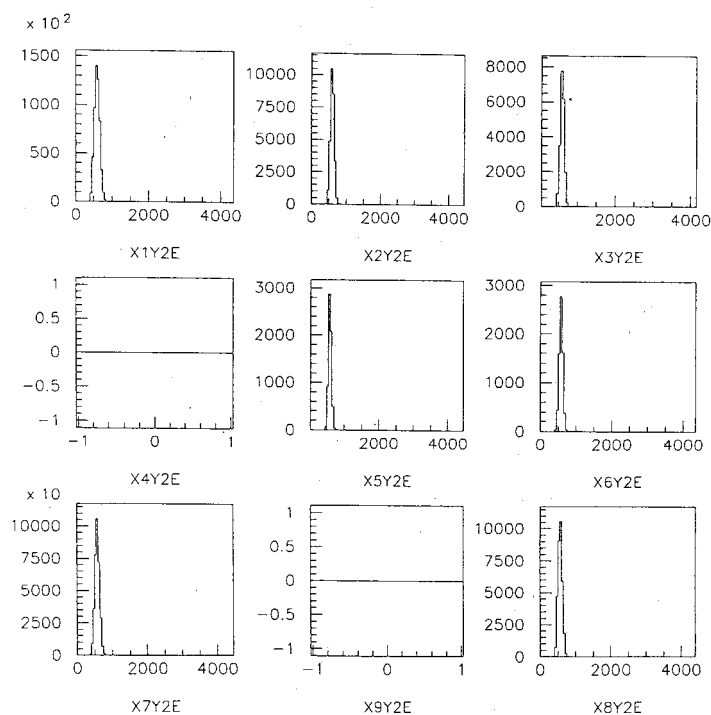


Figure 2. Spectra of 9 HgI₂ detectors on Column 2 for DOY 172 1997 and observing window number 3. Y-axis are counts in 2940 seconds and X-axis is the channel number.

of HgI₂ detector columns. After three weeks of columns and thresholds testing combinations, it became clear that switching off a particular column did not reduce the high HgI₂ count ratios in the others. The problem showed off in nearly all the columns and individual detectors. The HgI₂ count ratios not only saturated the onboard mass memory but also affected the count ratio of the two CdZnTe columns. The DPU was unable to manage the amount of data produced by the HgI₂ and consequently counts from the CdZnTe detectors were lost.

Finally, a decision was taken: to switch off seven columns of HgI₂ detectors. Only column no. 4, with the largest HgI₂ detectors was maintained on. The reason to maintain column no. 4 in operation was that, even presenting some instabilities, its count ratios did not saturate the telemetry. This detector plane configuration (171 cm² CdZnTe detectors and 9 HgI₂ with a useful collecting area of 4 cm²) has been maintained unchanged up to present. This decrease in the collecting area definitively jeopardize LEGRI capabilities as an astronomical instrument. The collecting area reduction in a factor 5 and the strong asymmetries introduced on the detector plane by the switching off of 7 columns of detectors drastically reduced LEGRI performances as an Imager (Ballesteros *et al.*, 1998). And LEGRI was, by this way, limited to a technology demonstrator for the CdZnTe detectors.

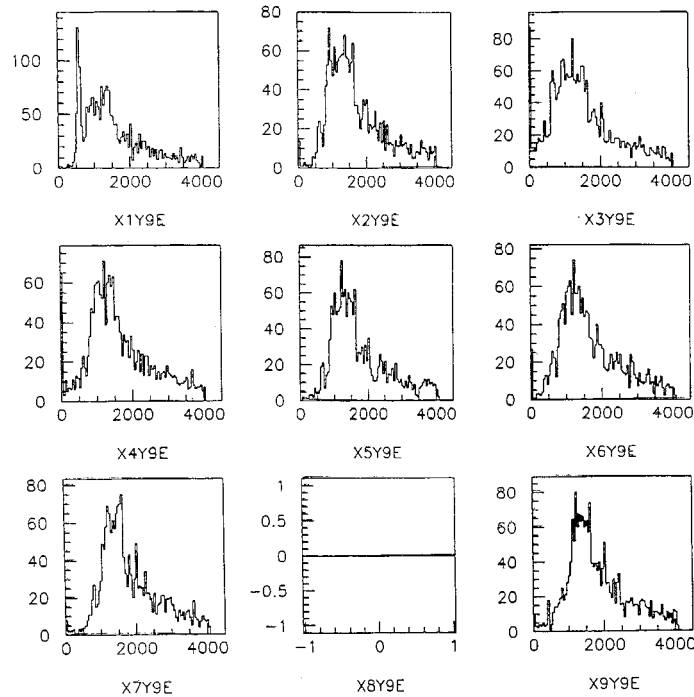


Figure 3. Spectra from the 8 CdZnTe detectors in Column 9 for DOY 172, 1997 and observing window number 3. Y-axis are counts in 2940 seconds and X-axis shows the channel number.

As a comparison with the HgI₂ spectra (Figure 2), the spectra of 8 CdZnTe detectors located in column no. 9 is displayed in Figure 3. These data correspond to the same observing period than those displayed in Figure 2 for the HgI₂. Detector no. 8 is the one lost during integration. Total count ratios are very similar in all of them except for detector X1Y9, which presents signatures of electronic noise at channel 500.

4. Standard Operational Mode. Detector Stability

The remainder 17 CdZnTe and 9 HgI₂ detectors with fixed thresholds (151 and 150) have been in operation from the end of the IOC up to now. To check the individual detector CdZnTe stability, data from 9 days of background measurements in 1997 have been analysed. It is not an easy task since the orbit of the MINISAT-01, crossing 8 times every day the South Atlantic Anomaly (SAA), induces very high and variable count ratios on the detectors during and after the transit.

During the SAA transit the count ratio raises in a factor 20 with respect to its minimum values. For transits crossing SAA close to center, when the satellite leaves it, the induced radioactivity, generated by the interaction or trapped protons

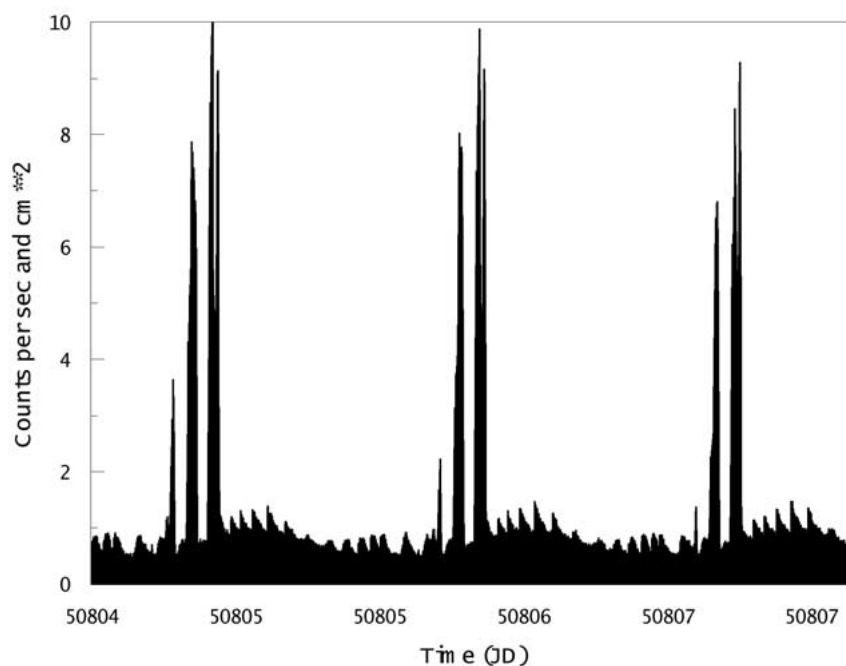


Figure 4. Count ratios for 17 CdZnTe detectors versus time for the DOY 356, 357, 358, 359, 1997. Very high count ratios for observations during SAA transits (3) and activated decays after transits are clearly seen.

during transits, is present for the rest of the orbit. For marginal transits the time needed to cool down the detectors is less than one orbit. At the same time, the effect of the Earth geomagnetic shielding is superimposed, this effect varies with the geomagnetic latitude. For a typical LEGRI observing window, the geomagnetic modulation induces count ratio variations also in a factor 2 corresponding to L-shell values between 1.1 and 1.9.

All these effects can be seen in Figure 4. We have plotted the background observations for four Christmas 1997 days (DOY 356-7-8-9). During this period LEGRI was kept on observing mode in some transits (3) through the SAA every day. X-axis is time in Julian Days and Y-axis are counts per cm^2 and per second. Figure 4 displays quite well the different LEGRI operative scenarios: crosses throughout the SAA with count ratios up to $11 \text{ counts sec}^{-1} \text{ cm}^{-2}$, activated periods after transits (fast decay) in which the background do not reach its minimum value, and finally geomagnetically modulated regions corresponding to observing windows after the last SAA passage, with count ratios varying between 0.5 and 1 count per second.

For the stability analysis we have checked in 9 background days (DOY 179, 198, 201, 219, 240, 356, 357, 258 and 359), observing windows before transits throughout the SAA. The data in 60 sec bins for every individual detector were compared to the column average value (9 detectors in C-0 and 8 detectors in C-9).

TABLE I

CdZnTe detector relative count ratios for the full LEGRI energy range. The first digit indicates the column number and the second digit the detector number

Detector number	01	02	03	04	05	06	07	08	09
DOY 356	1.82	1.05	0.96	1.00	0.97	0.95	0.99	1.01	1.08
DOY 357	1.79	1.02	0.98	0.96	0.96	1.02	0.99	0.97	1.10
DOY 358	1.83	1.01	0.97	1.01	0.96	1.03	0.98	0.94	1.11
DOY 359	1.76	0.99	0.98	0.97	0.99	0.97	1.01	1.01	1.11
Average	1.80	1.02	0.97	0.98	0.97	0.99	0.99	0.98	1.1
Sigma	0.03	0.02	0.01	0.02	0.01	0.03	0.01	0.03	0.02
DOY 201-219-198-179-240	2.0	1.04	1.01	0.97	0.97	0.99	0.98	1.0	1.06
Delta	0.2	-0.02	0.04	0.01	0.00	0.00	0.01	-0.02	-0.04
Detector number	91	92	93	94	95	96	98	99	
DOY 356	0.99	0.92	1.06	0.95	0.98	0.93	1.06	1.12	
DOY 357	1.04	0.98	0.99	0.95	0.96	0.94	1.02	1.11	
DOY 358	1.01	0.98	1.04	0.94	0.97	0.95	1.00	1.10	
DOY 359	1.03	0.98	1.00	0.99	0.92	0.95	1.02	1.11	
DOY 356-7-8-9	1.02	0.96	1.02	0.96	0.96	0.94	1.03	1.10	
Sigma	0.02	0.03	0.03	0.02	0.02	0.01	0.02	0.01	
DOY 201-219-198-179-240	1.03	0.97	1.02	0.95	0.95	0.94	1.04	1.12	
Delta	-0.01	-0.01	0.00	0.01	0.01	0.00	-0.01	-0.02	

In Table I, the results for the different detectors in detector columns (0 and 9) as a % of the the daily average, with indication of the DOY considered, are given. Standard deviation of the averages for four consecutive days (356-9) is at the level of 2%. Standard deviations and detector responses are identical for detectors located in C-0 and C-9. No systematic effects have been found between both columns. Only detector 01 deviates from this trend, which presents count ratios 1.8 times larger.

In Table I the averages for the other five days of 1997 background measurements are also given. Their values are in good agreement with those obtained in the 1997 Christmas time period. Deviations are also displayed in the last rows. All of them

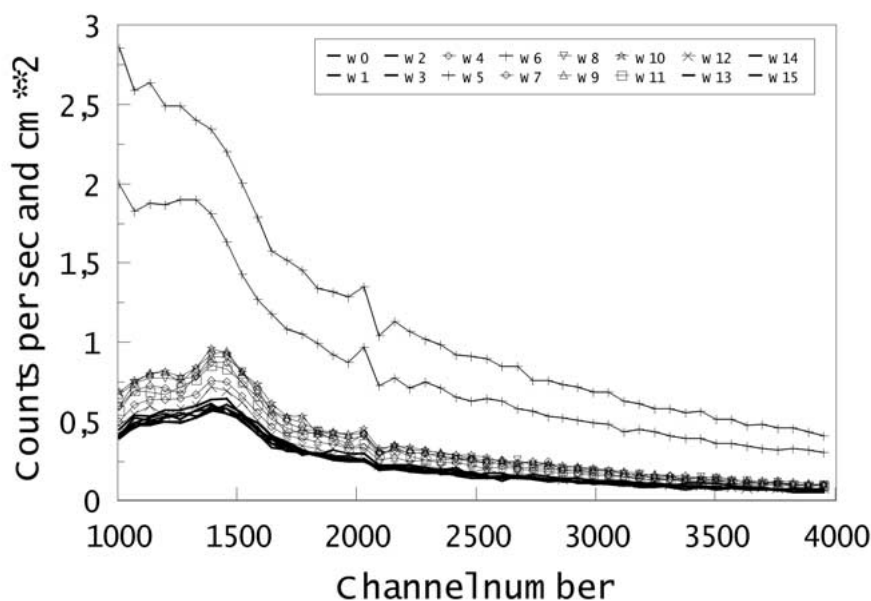


Figure 5. Background spectra for 16 observing windows in the DOY 356, 1997. Y-axis are counts per sec and cm^2 and X-axis is the channel number.

are within the uncertainties of the averages, except for detector 01, which presents significant deviations five times larger. As a conclusion, the CdZnTe detector count ratios present a remarkable stability all over the period considered (5 months) with variations in their relative count ratios of 2%. This applies for the total count ratios in the LEGRI full energy range (channels 1000 to 4000). Equivalence between channels and energy will be discussed further below.

For same days and observing windows, the minimum count ratios corresponding to observations very close to the geomagnetic equator ($L \sim 1$) and for geomagnetically modulated regions, have been also analysed. Their values show a remarkable stability as well as a good agreement with our theoretical predictions. (See Porras *et al.*, 2001, this volume). Finally, the geomagnetic modulation has been modelled in terms of both its dependence on the L-shell parameter and rigidity cut-off R_c . Results are discussed in Sanchez *et al.* (2001, this volume).

To conclude this section on detector stability analysis, we would point out some comments about the background spectra. For this purpose we have analysed the background spectra by using the same days already used for the discussion on detector total count ratio stability. Figure 5 displays the spectra of the CdZnTe detectors as a function of the energy channel for the 15 observing windows of DOY 356 1997.

Windows 0, 1, 2, 3, 13, 14 and 15 correspond to observing periods before the starting of the SAA transits or without recent crosses through it. Their background

spectra are dominated by the long-lived radioactivity decays and cosmic ray interactions modulated by the geomagnetic field (geomagnetically modulated regions). Their spectra (continuous lines) are equally shaped and very close in their absolute values. Differences between the absolute values are induced by small differences in their individual L-shell parameter values.

Oppositely, the spectra for windows 7 to 12 present higher count-ratios while maintaining the spectral shape. These windows correspond to periods immediately after SAA passages and include some mid-lived radioactivity decays (see below for a further discussion). Finally, the spectra corresponding to windows 5 and 6 (labelled by crosses and continuous lines) come from data obtained during the SAA passage itself. Direct interaction of trapped protons and short-lived radioactivity decays (less than 1 min) increases the counting ratio in all the channels and changes the background spectral shape.

To analyse the spectral shape changes, we defined a Reference Spectra (RS) by using the data for observing windows without recent crosses through the SAA (W0-1-2-3-13-14-15). These count ratios come mainly from cosmic interactions and long term radioactivity decays from trapped particles. Ratios between Individual Spectra vs Reference Spectra are displayed in Figure 6, labelled with different symbols and with indication of the observing window number considered. For all the windows, except windows 5 and 6, which correspond to SAA transits, the ratios present a flat structure, moving up and down depending on both the L-shell parameter and the doses received during the transit before starting observations. For windows 5 and 6 the ratios are absolutely different. Both high and low energy parts of the spectra raise very fast, presenting a minimum around channel 1500 (60 KeV). The short-lived radioactivity decays and proton direct interactions are responsible for the observed changes in the spectral shapes.

This background spectral behaviour has been tested also by using the 9 days of background observations considered for the detector stability analysis. No differences have been found with respect to the particular case discussed above (DOY 356).

The CdZnTe detector background spectra presents the same shape for all the observing windows, varying only their absolute values as a function of both previous crosses throughout the SAA (proton doses received) and L-shell parameter values. Long-lived radioactivity decays and cosmic ray interactions dominate the background spectra. When LEGRI crosses the SAA, the background spectra during transit present a completely different shape according to the one discussed above in DOY 306. These spectral features show no change during the last three years of LEGRI operations.

With the data of the 4 consecutive days of background measurements (356-9) and for observing periods well outside the main SAA crosses, we have defined the average background spectra for a mean L-shell value of 1.49. By using the second order fit discussed in Sanchez *et al.* (2001, this volume), we have computed the Reference Background Spectrum (RBS) at the geomagnetic equator ($L = 1.1$).

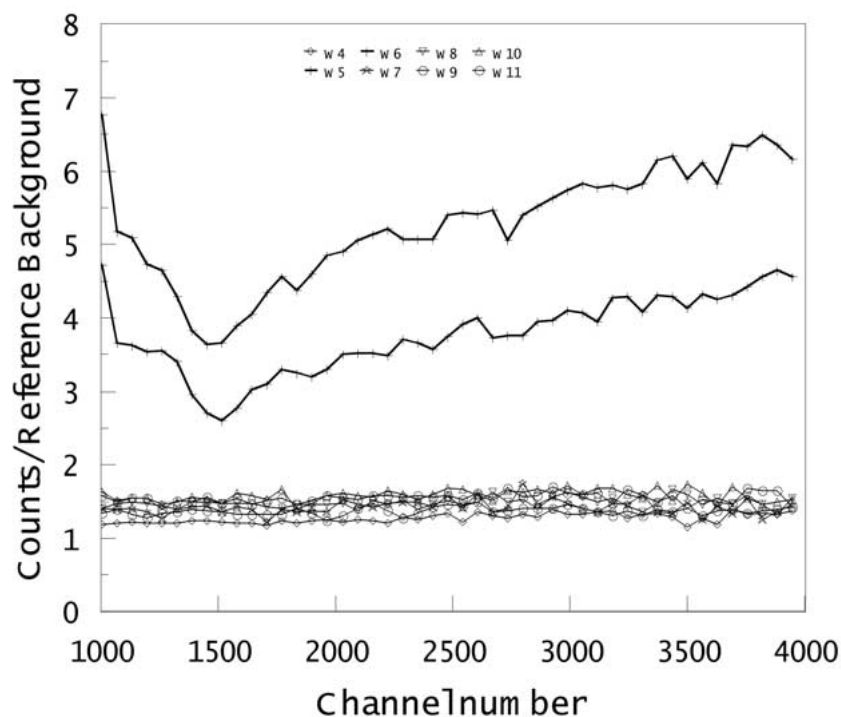


Figure 6. Background Spectra/ Background Reference Spectra ratios at L-shell minimum for 8 observing windows for the DOY 356, 1997. Y-axis are counts/reference Spectra counts and X-axis is the channel number.

This is the background spectrum used to analyse the Crab observations in the next section.

5. Detector Calibration. Ground and Crab

The CdZnTe detectors were calibrated in two steps before launch: first at the University of Birmingham just after Detector Unit integration, and later at CASA during the LEGRI integration on the Minisat-01 payload module. Three radioactive sources were used: ^{241}Am , ^{109}Cd and ^{133}Ba , covering an energy range between 16 KeV and 80 KeV. Different combinations of thresholds were tested in the neighbourhoods of the flight values (151). For this particular threshold the 16 KeV ^{241}Am peak was not seen, indicating a LEGRI lower energy threshold of 20 KeV or a little bit larger.

For the operational LEGRI threshold (151), the CdZnTe detector calibration follows a linear law:

$$E(\text{KeV}) = -60.5 + 0.081 \text{ channel-number (with } r=99\% \text{ and sigma}$$

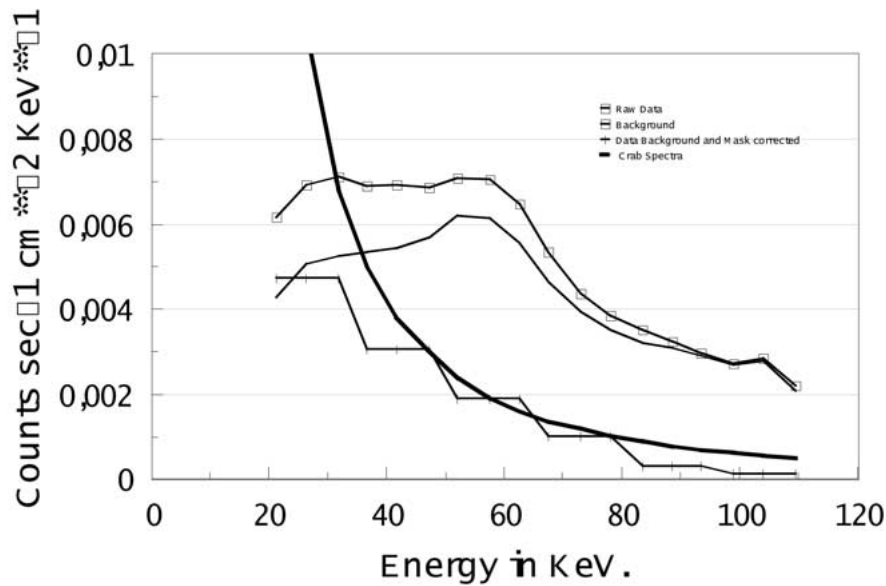


Figure 7. Crab observations in DOY 254, 255 and 256, 1997 (28569 seconds) with the Crab in the LEGRI FOV centre. The continuous line is the averaged Crab published spectra.

of the residuals equal to 24)

The energy resolution found was 16 KeV.

For in orbit calibration, one whole month in 1997 was devoted to Crab observations. We selected three days of observation having the Crab in the centre of the LEGRI FOV (DOY 254-55-56). For these days only observing windows before the start of the SAA transits were used to avoid background fast changes during transits and strong decay regions. Total integration time was 28.569 seconds.

The background was subtracted from the raw data by using the Reference Background Spectrum discussed in previous sections. Raw data was also corrected for the L-shell values computed for the different observing windows during Crab observations. In Figure 7 raw LEGRI data (squares + continuous line) and the background spectrum (continuous line) are displayed. X-axis is energy in KeV and Y-axis are counts $\text{cm}^2 \text{sec}^{-1}$ and KeV. The bin used is 15 KeV, which corresponds to the LEGRI CdZnTe spectral resolution previously discussed. Last step before comparing Crab data to the Crab fluxes from the literature is to correct them for the mask opacity effect. The Crab observed spectra (background and mask corrected) is displayed in Figure 7 labelled by a continuous line + crosses.

To compare these observations to previous total Crab published fluxes, we have averaged the spectra of HEAO4 (Jung, 1989), POKER (Ubertini, 1994) and LEGS (Hameury *et al.*, 1983) taken from the compilation of Macomb and Gehrels, 1999. Residuals Crab average minus Crab observed by LEGRI are also displayed by a dashed line (15 KeV resolution). The agreement between LEGRI observations and

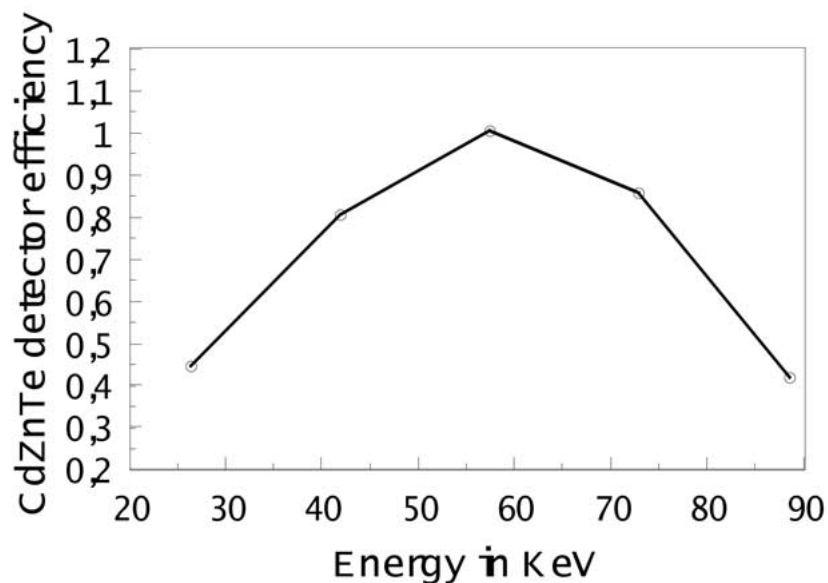


Figure 8. CdZnTe detector plane efficiency versus energy.

Crab average is quite good for energies between 30 and 90 KeV. For energies below 30 the effects of the non-linearity on the threshold used is clearly seen.

Detector efficiencies have been computed as the ratio between LEGRI Crab data / Crab published data and are plotted in Figure 8. At the lower LEGRI energy band (25 ± 7.5 KeV) the detector efficiency is at the level of 45% indicating effects of the threshold non-linear cuttings. For energies between 40 and 70 KeV, LEGRI efficiency approaches the unit (90%). For energies higher than 70 KeV efficiency drops very quickly, approaching 40% at the end of LEGRI energy calibrated range.

6. Routine Operations

Since the end of the LEGRI IOC and Crab observations in September 1997 until mid 1999, LEGRI has been in operation continuously by scanning the Galactic Plane in three main regions: the Cygnus region (from Cyg X1 to Cyg X2), the Crab region, and the sky close to the Ecliptic Pole from SMC X-1 to Cir X-1.

The Galactic Centre was pointed for the first time in September 1999. In Figure 9 the centroids of LEGRI pointings for 1998 are plotted. To understand Figure 9 we need to take into account that the LEGRI FCFOV is quite large, 22 degrees, which implies a large area coverage for every exposure, much larger than the one indicated in Figure 9.

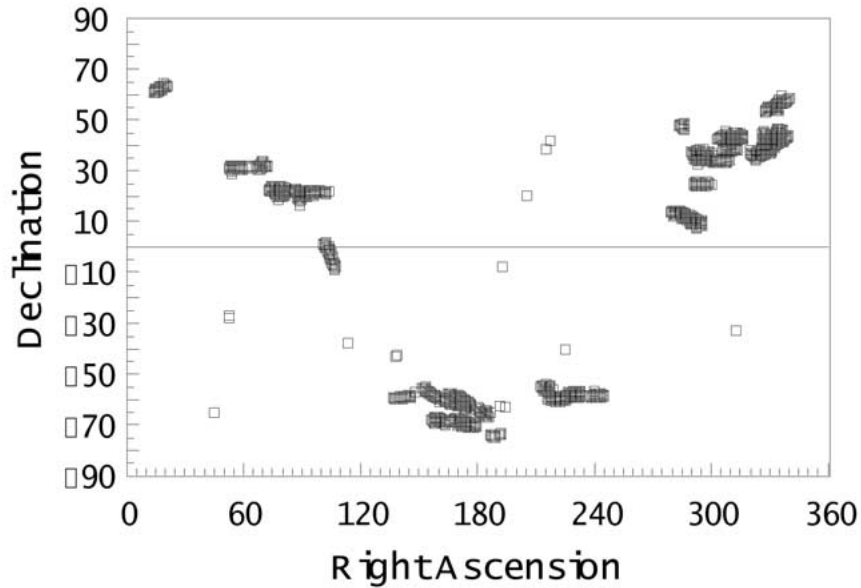


Figure 9. LEGRI pointings in 1998.

7. Conclusions

LEGRI as a system is working since its first switched-on in May 1997 within its design parameters. Housekeeping data show a very remarkable stability for the full system. The Star Sensor daily provides useful data for pointing reconstruction purposes.

The operational 17 CdZnTe detectors have demonstrated their capability to survive strong proton fluxes without damage. One orbit (1.5 h) after the last SAA transit, they recover their count ratio without changes. Minimum count ratios at the geomagnetic equator are stable after 2 years of operation and in very good agreement with our theoretical estimations. Background spectral shapes are unchanged after 2 years of space operations and in good agreement with our theoretical predictions.

Oppositely, 70 out of the 80 HgI₂ detectors have been switched off in the earliest days of LEGRI operation. Very fast saturation on the mass memory allocated to LEGRI together with the impact on the observed count ratios on the rest of the detectors imposed their switched off. The remaining column of HgI₂ detectors is still in operation but it presents also remarkable instabilities.

The loss of an 80% of the detector plane jeopardised the LEGRI capabilities as an astronomical instrument. We can perform only observations of gamma ray emitters at the 100 mCrab level larger in non crowded fields. The imaging capabilities have been also dramatically reduced.

LEGRI has been providing very useful data about background modelling validation and geomagnetic mapping at 574 km altitude for the last two years of operation. The most striking result might be the demonstration of the CdZnTe detectors capability to survive in space without degradation after strong proton doses.

Acknowledgements

We would like to thank all the institutions and groups supporting LEGRI development and operation, with special attention to the unvaluable contribution of the University of Birmingham colleagues and INTA staff. This work has been partially supported by the Spanish *Comision Interministerial de Ciencia y Tecnología* (CICYT) under grant ESP98-1572-E, and the *Generalitat Valenciana* (IMPIVA).

References

- Ballesteros, F., Sánchez, F. and Reglero, V.: 1998, *Nuclear Instrumentation and Methods B*, **145**, 3.
- Ballesteros, F., Bernabeu, G., Gimenez, A., Fabregat, J., Perez, F., Porras, E., Reglero, V., Reig, P., Robert, A., Saenz, A., Sánchez, F., Díaz, E., Martín, J.A., Reina, M., Sánchez, A., Torralbo, J., González, M., Marín, J., Martínez, L., Olmos, P., Pérez, J.M., Cruise, M., Swinyard, B.M., Eyles, C., Skinner, J., Bird, A.J., Dean, A.J. and Chuantaure, H.S.: 1995, *Imaging in High Energy Astronomy*, Ed. L. Bassani and G. di Cocco, 183.
- Blay, P., Suso, J., Robert, A., Requena, J.L., Alamo, G. and Reglero, V., this issue.
- Hameury, J.M., *et al.*: 1983, *ApJ*, **270**, 144.
- Jung, G.V.: 1989, *ApJ*, **338**, 972.
- Macomb, D.J. and Gehrels, N.: 1999, *ApJ SS*, **120**, 335.
- Perfect, C., Bird, A.J., Dean, A.J., Ferguson, C., Lei, F. and Lockley, J.J.: 2001, this volume.
- Porras, E., Reglero, V. and Sanchez, F.: 2001, this volume.
- Reglero, V., Sánchez, F., Ballesteros, F., Porras, E., Pérez, F. and Robert, A., 1997, ESA SP-382, 343.
- Sanchez, F. and Reglero, V.: 2001, this volume.
- Suso, J., Blay, P., Robert, A. and Reglero, V.: 2001, this volume.
- Ubertini, P.: 1994, *ApJ*, **421**, 269.

